Pure Appl. Chem., Vol. 81, No. 4, pp. 649–665, 2009.
doi:10.1351/PAC-CON-08-08-27
© 2009 IUPAC

Proton transfers in aromatic systems: How aromatic is the transition state?*

Claude F. Bernasconi

Department of Chemistry and Biochemistry, University of California, Santa Cruz, CA 95064, USA

Abstract: The question as to what extent aromaticity in a reactant or product is expressed in the transition state of a reaction has only recently received serious attention. Inasmuch as aromaticity is related to resonance, one might expect that, in a reaction that leads to aromatic products, its development at the transition state should lag behind bond changes as is invariably the case for the development of resonance in reactions that lead to delocalized products. However, recent experimental and computational studies on proton transfers from carbon acids suggest the opposite behavior, i.e., the development of aromaticity at the transition state is *more* advanced than the proton transfer. The evidence for this claim is based on the determination of intrinsic barriers that show a decrease with increasing aromaticity. According to the Principle of Nonperfect Synchronization (PNS), this decrease in the intrinsic barrier implies a disproportionately large amount of aromatic stabilization of the transition state. Additional evidence for the high degree of transition state aromaticity comes from the calculation of aromaticity indices such as HOMA, NICS, and the Bird Index. Possible reasons why the degree to which aromaticity and resonance are expressed at the transition state is different are discussed.

Keywords: proton transfer; aromaticity; transition state imbalance; principle of nonperfect synchronization.

INTRODUCTION

There is increasing recognition among physical organic chemists that the most appropriate and useful kinetic measure of chemical reactivity is the *intrinsic* barrier ($\Delta G_o^{\ddagger}$) rather than the actual barrier ($\Delta G^{\ddagger}$), or the *intrinsic* rate constant (k_o) rather than the actual rate constant (k) of a reaction [1,2]. They represent the barrier (rate constant) in the absence of a thermodynamic driving force ($\Delta G^o = 0$) and are either obtained by interpolation or extrapolation of kinetic data, or by applying the Marcus equation [1]. For example, for solution-phase proton transfers from carbon acids to buffer bases, eq. 1, k_o may be determined from Brønsted plots of log k_1 or log k_{-1} vs. log K_1 ($K_1 = k_1/k_{-1}$) by interpolation or extrapolation to log $K_1 = 0$, while $\Delta G_o^{\ddagger}$ can be calculated from k_o via the Eyring equation.

(1)

*Paper based on a presentation at the 19th International Conference on Physical Organic Chemistry (ICPOC-19), 13–18 July 2008, Santiago de Compostela, Spain. Other presentations are published in this issue, pp. 571–776.

For the last 25 years, a major thrust of our research has been to examine the factors that contribute to the intrinsic barriers of reactions, with a strong focus on the question as to what extent reactant and/or product stabilizing (or destabilizing) factors are expressed at the transition state and how this affects the intrinsic barrier. We have shown that a particularly appropriate framework for analyzing these effects is provided by the Principle of Nonperfect Synchronization (PNS) [3]. This principle states that any product-stabilizing factor whose development lags behind bond changes at the transition state, or any reactant-stabilizing factors whose loss at the transition state is ahead of bond changes, increases the intrinsic barrier or decreases the intrinsic rate constant. For product-stabilizing factors that *develop ahead* of bond changes, or reactant stabilizing factors *whose loss lags behind* bond changes, the effect is reversed, i.e., there is a decrease in $\Delta G_o^{\ddagger}$ or an increase in k_o. What makes the PNS particularly useful is that it is completely general, mathematically provable, and knows no exceptions [3c].

The study of proton transfers from carbon acids activated by π-acceptors (Y in eq. 1) has played a particularly prominent role in illustrating the manifestations of the PNS [3–7], but there exist numerous examples of other types of reactions whose structure–reactivity behavior was successfully analyzed in terms of the PNS [3,8–11]. Among the many factors examined, the nature of the π-acceptor Y has been shown to often have the largest impact on the intrinsic barrier, at least in solution-phase reactions where the intrinsic barrier increases with increasing charge delocalization in the anion. This is because delocalization invariably lags behind proton transfer at the transition state as represented, in exaggerated form, in **1**; this lag is often referred to as a transition state imbalance [1,12]. Since delocalization is a product-stabilizing factor, the result, according to the PNS, must be an increase in $\Delta G_o^{\ddagger}$. Table 1 lists a number of representative examples which show the trend toward higher $\Delta G_o^{\ddagger}$ or lower k_o values with increasing π-acceptor strength of Y.

1 **2**

Table 1 Representative intrinsic rate constants and intrinsic barriers for proton transfers from carbon acids to secondary alicyclic amines.

C–H acid	Solvent[a]	Log k_o [b]	$\Delta G_o^{\ddagger}$ (kcal/mol)	Ref.
HCN	H_2O (20 °C)	ca. 8.6	ca. 5.6	c
$CH_2(CN)_2$	H_2O (25 °C)	ca. 7.0	ca. 7.8	d
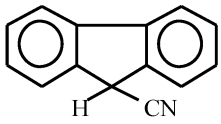	50 % DMSO (20 °C)	4.58	10.9	e
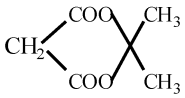	50 % DMSO (20 °C)	3.90	11.9	f
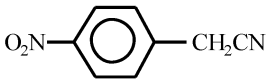	50 % DMSO (20 °C)	3.70	12.1	g
$(CO)_5Cr{=}C(OMe)CH_3$	50 % MeCN (25 °C)	3.52	12.6	h
$CH_2(COCH_3)_2$	50 % DMSO (20 °C)	2.75	13.4	i
$(CO)_5Cr{=}C(OMe)CH_2Ph$	50 % MeCN (25 °C)	1.86	14.6	h
CH_3NO_2	50 % DMSO (20 °C)	0.73	16.1	j
$PhCH_2NO_2$	50 % DMSO (20 °C)	–0.25	17.4	j

[a]50 % DMSO is 50 % DMSO/50 % water (v/v); 50 % MeCN is 50 % MeCN/50 % water (v/v).
[b]In units of M^{-1} s^{-1}.
[c]R. A. Bednar, W. P. Jencks. *J. Am. Chem. Soc.* **107**, 7117, 7126 (1985).
[d]F. Hibbert. *Compr. Chem. Kin.* **8**, 97 (1977).
[e]C. F. Bernasconi, F. Terrier. *J. Am. Chem. Soc.* **109**, 7115 (1987).
[f]Ref. [3c].
[g]C. F. Bernasconi, S. A. Hibdon. *J. Am. Chem. Soc.* **105**, 4343 (1983).
[h]C. F. Bernasconi, W. Sun. *J. Am. Chem. Soc.* **115**, 12526 (1993).
[i]C. F. Bernasconi, R. D. Bunnell. *Isr. J. Chem.* **26**, 420 (1985).
[j]C. F. Bernasconi, D. A. V. Kliner, A. S. Mullin, J. X. Ni. *J. Org. Chem.* **53**, 3342 (1988).

Solvation can also have a significant effect on intrinsic barriers or intrinsic rate constants. A number of representative examples are reported in Table 2. The largest solvent effect is found for the formation of nitronate ions because their solvation by hydrogen bonding in hydroxylic solvents is particularly strong. Inasmuch as solvation also lags behind proton transfer at the transition state (**1** vs. **2**), there is again an increase in the intrinsic barrier or a decrease in k_o with increasing solvation as seen when increasing the water content of the solvent. In cases where the negative charge is more delocalized, the hydrogen bonding solvation is weaker and the solvent effect smaller, as is the case for the deprotonation of acetylacetone. When the anionic charge is very highly dispersed, hydrogen bonding solvation becomes negligible and with it the solvent effect on k_o, as in the deprotonation of 9-cyanofluorene; in this case solvation by dimethyl sulfoxide (DMSO) becomes more effective than solvation by water and k_o is slightly higher in water than in 90 % DMSO.

Table 2 Representative intrinsic rate constants for proton transfers from carbon acids to secondary alicyclic amines in different solvents.

C–H acid	Log k_o			Ref.
	H_2O	50 % DMSO/50 % H_2O	90 % DMSO/10 % H_2O	
CH_3NO_2	–0.59	0.73	3.06	a
$PhCH_2NO_2$	–0.86	–0.25	1.75	a
$CH_2(COCH_3)_2$	2.60		3.64	b
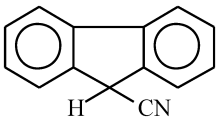	4.58		4.40	c

[a]C. F. Bernasconi, D. A. V. Kliner, A. S. Mullin, J. X. Ni. *J. Org. Chem.* **53**, 3442 (1988).
[b]C. F. Bernasconi, R. D. Bunnell. *Isr. J. Chem.* **26**, 420 (1985).
[c]C. F. Bernasconi, F. Terrier. *J. Am. Chem. Soc.* **109**, 7115 (1987).

A consequence of the transition state imbalance is that the inductive effect of substituents other than Y may either increase or decrease the intrinsic barrier, depending on their location within the molecule. For example, if an electron-withdrawing substituent X is attached to the carbon with the acidic proton or to a group attached to that carbon, eq. 2, its effect is to decrease $\Delta G_o^{\ddagger}$.

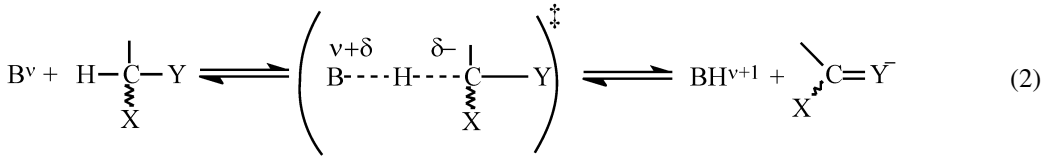

(2)

This is because there is a disproportionately strong stabilization of the transition state compared to that of the carbanion due to the closer proximity of X to the charge at the transition state. A manifestation of this effect is seen in the Brønsted coefficients of the reactions of **3** [13,14] and **4** [15] with buffer bases. In both cases, α determined by varying the substituent in the phenyl group exceeds the value β obtained by varying the buffer base.

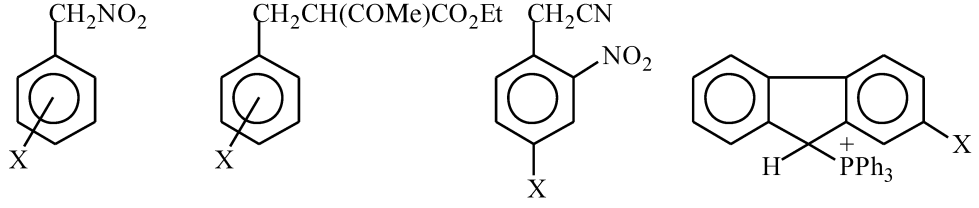

3 **4** **5** **6**

In contrast, when an electron-withdrawing substituent is attached to the Y-group, eq. 3, the result is an *increase* in the intrinsic barrier because it is the carbanion rather than the transition state that

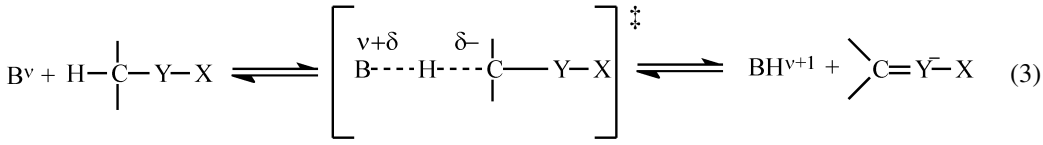

(3)

enjoys a disproportionately strong stabilization due to the closer proximity of X to the charge in the anion. In this case, the Brønsted α value is *smaller* than the β value, as seen for the reactions of **5** [16] and **6** [17] with amines.

Regarding the inductive effect of the Y-group, its influence on solution-phase proton transfers is difficult to evaluate based on experimental observations because the π-acceptor effect of Y usually dominates. However, in gas-phase identity proton transfers of the type shown in eq. 4 (Y = CN, C≡CH, $CH{=}CH_2$, CH=O, CH=S, CH=NH, NO_2, NO) there is a strong decrease in the intrinsic barrier, $\Delta H_o^{\ddagger}$,

$$Y{-}CH_3 + CH_2{=}Y^- \rightleftharpoons \left[Y{-}\overset{\delta-}{C}H_2\cdots\overset{\delta+}{H}\cdots\overset{\delta-}{C}H_2{-}Y\right]^{\ddagger} \rightleftharpoons {}^-Y{=}CH_2 + CH_3{-}Y \qquad (4)$$

with increasing electron withdrawing strength of Y [18]. In fact, this barrier-reducing effect is stronger than the barrier increase due to the π-acceptor effect which leads to a net reduction of the intrinsic barrier by Y relative to the reaction $CH_4 + CH_3^- \rightleftarrows CH_3^- + CH_4$. The strong transition state stabilization by the inductive effect appears to be related to the high negative charges (–0.60 to –0.65) on each of the two CH_2Y fragments of the transition state, which is partially due to the substantial positive charge (0.25–0.30) on the proton in flight.

Another factor that reduces intrinsic barriers or increases k_o is the polarizability of a substituent X (eq. 2) or Y (eq. 4). For example, in water k_o for the deprotonation of $PhSCH_2NO_2$ by secondary cyclic amines is 151-fold higher than that of $PhCH_2CH_2NO_2$ while in 90 % DMSO/10 % water, the difference is a factor of 37 in favor of the more polarizable sulfur compound [19]. The reason for the increase in k_o is similar to that with the inductive effect of X, i.e., the closer proximity of X to the charge at the transition state compared to that in the anion. In the reactions of eq. 4, the polarizability effect manifests itself most strongly in the $CH_2CH{=}S/CH_2{=}CH{-}S^-$ system [18].

EFFECT OF REACTANT AND PRODUCT AROMATICITY ON INTRINSIC BARRIERS

The question as to what extent aromaticity in a reactant or product is expressed in the transition state of a reaction has only recently received serious attention. Inasmuch as aromaticity is related to resonance, one might expect that its development at the transition state should also lag behind bond changes (or its loss from a reactant would be ahead of bond changes) and hence lead to an increase in $\Delta G_o^{\ddagger}$, as is the case for resonance/delocalized systems. However, recent experimental and computational studies from our laboratory suggest the opposite behavior. In the remainder of this paper, the evidence for this conclusion and possible reasons why the degree to which aromaticity and resonance are expressed at the transition state is different will be discussed.

Experimental studies

The first system that showed a decrease in the intrinsic barrier or increase in the intrinsic rate constant is the deprotonation of cationic rhenium Fischer carbene complexes leading to the formation of derivatives of the aromatic heterocycles furan, selenophene, and thiophene (eq. 5) [20]. The increase in aromaticity along the order **7-O** < **7-Se** < **7-S** is reflected in the pK_a values of **7H$^+$-X** determined in

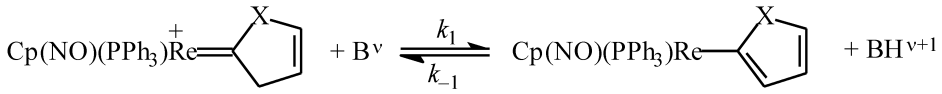

7H$^+$-O (X = O)
7H$^+$-Se (X = Se)
7H$^+$-S (X = S)

7-O (X = O)
7-Se (X = Se)
7-S (X = S)

(5)

50 % MeCN/50 % water: 5.78 (X = O), 4.18 (X = Se), 2.50 (X = S). Intrinsic rate constants for proton transfer to primary aliphatic amines, secondary alicyclic amines, and carboxylate ions are summarized in Table 3. The order of the intrinsic rate constants k_o(X = O) < k_o(X = Se) < k_o(S) for each buffer family is the same as the aromaticity order, i.e., k_o increases with increasing aromaticity of **7-X**.

Table 3 Intrinsic rate constants for proton transfer from rhenium carbene complexes (**7H$^+$-X**) to buffer bases in 50 % MeCN/50 % water (v/v) at 25 °C.[a,b]

Carbene complex	pK_a^{CH}	Log k_o (RNH_2)	Log k_o (R_2NH)	Log k_o (RCO_2^-)
7H$^+$-O	5.78	–0.83	–0.46	–0.01
7H$^+$-Se	4.18	0.14	0.92	0.72
7H$^+$-S	2.50	0.27	1.05	1.21

[a]k_o in units of M^{-1} s^{-1}.
[b]From ref. [20].

The second system showing the same qualitative results is that of eq. 6 [21]. Table 4 summarizes pK_a^{CH} values and intrinsic rate constants for the reactions with primary aliphatic and secondary alicyclic

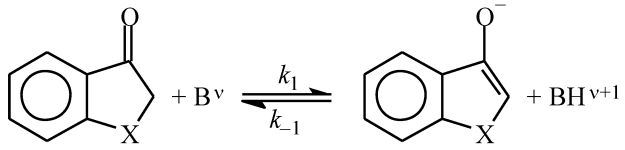

8H-O (X = O)
8H-S (X = S)

8$^-$-O (X = O)
8$^-$-S (X = S)

(6)

amines. Another system, eq. 7, yielded somewhat ambiguous results stemming from complications due to resonance effects in **9H-X** [22]; however, a detailed analysis revealed that here again the greater aromaticity of the sulfur derivative increases k_o relative to the oxygen derivative [21].

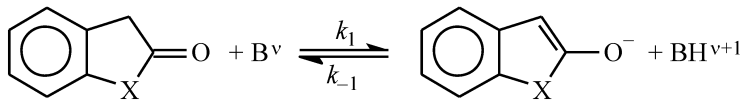

9H-O (X = O)
9H-S (X = S)

9$^-$-O (X = O)
9$^-$-S (X = S)

(7)

Table 4 Intrinsic rate constants for proton transfer from benzofuranone (**8H-O**) and benzothiophenone (**8H-S**) to amines in water at 25 °C.[a,b]

C–H acid	pK_a^{CH}	Log k_o (RNH_2)	Log k_o (R_2NH)
8H-O	11.72	1.16	1.64
8H-S	9.45	1.72	2.64

[a]k_o in units of M^{-1} s^{-1}.
[b]From ref. [21].

Computational studies

Our first study focused on two identity proton transfers involving the highly aromatic and prototypical benzene and cyclopentadienyl systems (eqs. 8a and 9a) [23]. Calculations at the MP2/6-311+*G*** level show a significantly lower $\Delta H_o^{\ddagger}$ for the more aromatic $C_6H_7^+/C_6H_6$ system (eq. 8a) compared to the

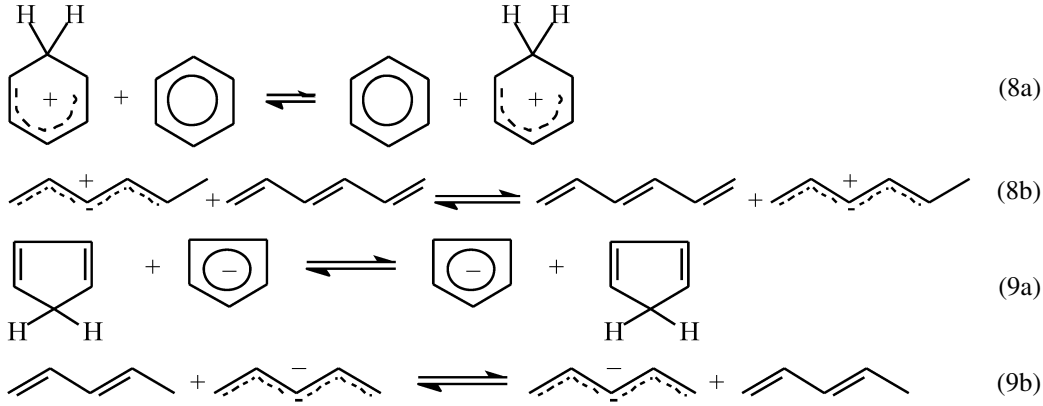

$C_5H_6/C_5H_5^-$ system (eq. 9a). A lowering of the intrinsic barrier due to aromaticity can also be deduced from a comparison between the $\Delta H_o^{\ddagger}$ values for the aromatic system and those for the corresponding noncyclic reference system, e.g., eq. 8a vs. 8b and eq. 9a vs. 9b. The numerical results of these calculations are summarized in Table 5. These results imply a disproportionately large aromaticity development at the transition state, i.e., the sum of the aromatic stabilization energies (ASEs) of the two halves of the transition state is greater than the ASE of the respective aromatic reactant/product. This is illustrated by the schematic energy profiles shown in Fig. 1 for reactions 8a/9a and 9a/9b, respectively. The arrows pointing down represent the aromatic stabilization energies of the reactants (ASE_R), products (ASE_P) and the transition state (ASE_{TS}), respectively. The greater than 50 % aromaticity in both halves of the transition state are reflected in the fact that $|ASE_{TS}| > |ASE_R| = |ASE_P|$.

Table 5 Intrinsic barriers ($\Delta H^{\ddagger}_{o}$) of reactions 8a, 8b, 9a, and 9b and aromatic stabilization energies (ASEs) in the gas phase.[a]

System	Eq.	ASE kcal/mol	$\Delta H^{\ddagger}_{o}$ kcal/mol	$\Delta\Delta H^{\ddagger}_{o}$ kcal/mol
$C_6H_7^+/C_6H_6$	8a	–36.3	–7.6	–11.1
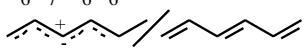	8b		3.5	
$C_5H_6/C_5H_5^-$	9a	–29.4	2.2	–7.6
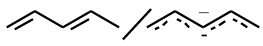	9b		9.8	

[a]At MP2/6-311+G**, ref. [23].
[b]$\Delta\Delta H^{\ddagger}_{o} = \Delta H^{\ddagger}_{o}$ (cyclic) – $\Delta H^{\ddagger}_{o}$ (noncyclic).

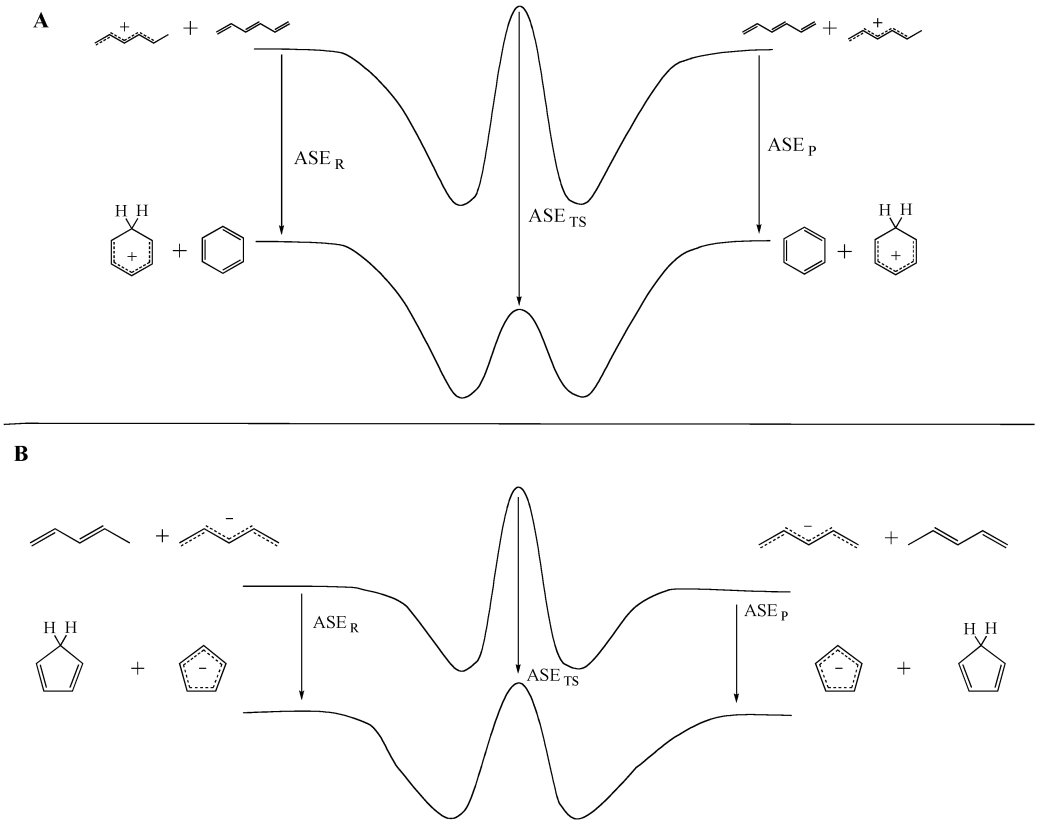

Fig. 1 Reaction energy profiles for reactions 8a/8b (**A**) and 9a/9b (**B**). Aromatic stabilization of the transition state is greater than that for benzene or cyclopentadienyl anion, respectively.

The conclusions based on energy calculations are supported by the calculation of aromaticity indices such as the harmonic oscillator model of aromaticity (HOMA) [24] and nucleus-independent chemical shift, NICS(1) [25] summarized in Table 6; they show that the change in these indices in going from reactants to the transition state relative to the change from reactants to products is significantly greater than 50 %.

Table 6 Aromaticity indices for the reactions of eqs. 8a and 9a in the gas phase.[a]

	HOMA	NICS(1)
$C_6H_7^+$	0.415	–6.05
TS	0.874	–9.26
C_6H_6	0.963	–10.20
% progress at TS[b]	83.8	77.3
C_5H_6	–0.791	–0.517
TS	0.560	–8.33
$C_5H_5^-$	0.739	–9.36
% progress of TS[b]	88.3	75.4

[a]At MP2/6-311+*G***, ref. [23].
[b][Index(TS) – Index(Reactant)]/[Index (Product) – Index(Reactant)] × 100.

Another study involved the identity reactions shown in eq. 10 [26]. Calculations at the MP2/6-31+*G*** level yielded a $\Delta H_o^{\ddagger}$ for X = S that is lower than for X = O. It was also found that $\Delta H_o^{\ddagger}$

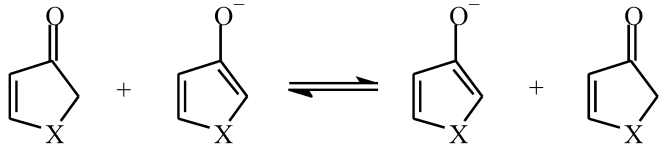

(10)

10H-O (X = O) **10**$^-$**-O** (X = O) **10**$^-$**-O** (X = O) **10H-O** (X = O)
10H-S (X = S) **10**$^-$**-S** (X = S) **10**$^-$**-S** (X = S) **10H-S** (X = S)

for the reactions of eq. 10 was lower than for the corresponding noncyclic reference systems of eq. 11. The results are summarized in Table 7. Furthermore, the intrinsic barrier for the deprotonation of **10H-S** by CN^- is lower than for the deprotonation of **10H-O** by the same base. All these results indicate that aromaticity lowers the intrinsic barrier and increasingly so with increasing aromaticity.

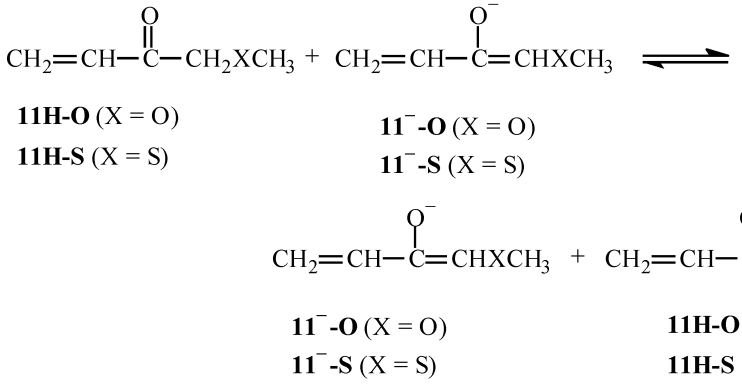

(11)

11H-O (X = O)
11H-S (X = S)

11$^-$**-O** (X = O)
11$^-$**-S** (X = S)

11$^-$**-O** (X = O)
11$^-$**-S** (X = S)

11H-O (X = O)
11H-S (X = S)

Table 7 Intrinsic barriers of reactions 10 and 11 in the gas phase.[a]

System	$\Delta H_o^{\ddagger}$ kcal/mol	$\Delta\Delta H_o^{\ddagger}$ [b] kcal/mol
10H-O/10⁻-O	3.6	–1.8
11H-O/11⁻-O	5.4	
10H-S/10⁻-S	2.3	–2.0
11H-S/11⁻-S	4.3	

[a]At MP2/6-31+*G***, ref. [26].
[b]$\Delta\Delta H_o^{\ddagger} = \Delta H_o^{\ddagger}$ (cyclic) – $\Delta H_o^{\ddagger}$ (noncyclic).

Further evidence showing disproportionately high transition state aromaticity comes from NICS values [25] and Bird Indices [27] as indicators of aromaticity. These aromaticity indices are summarized in Table 8 for the identity reactions (eq. 10). As was the case for reactions 8a and 9a, the progress in the development of aromaticity at the transition state is greater than 50 %.

Table 8 Aromaticity indices for the identity proton transfers of eq. 10.[a]

Species	NICS(–1)	Bird Index
10H-O	–2.47	22.68
TS	–5.46	36.76
10⁻-O	–6.74	40.28
% progress at TS	69.9	80.0
10H-S	–2.45	31.31
TS	–5.37	53.19
10⁻-S	–7.33	64.20
% progress at TS	59.8	66.5

[a]At MP2/6-31+*G***, ref. [26].

NICS and Bird Indices were also calculated for transition states of the reactions of **10H-O** and **10H-S** with a series of carbanions. The results are reported in Table 9. The trends in both parameters show a clear increase as the transition state becomes more product-like with increasing endothermicity, indicating an increase in transition state aromaticity. Even more revealing is the % progress at the transition state, which indicates that this progress is >50 % not only for the endothermic reactions (product-like transition states) but even for most of the exothermic reactions (reactant-like transition states) except those with strongly negative ΔH^{o} values.

Table 9 Transition state aromaticity indices for the reactions of **10H-O** and **10H-S** with carbanions in the gas phase.[a]

RC̄HY	ΔH^o kcal/mol	NICS(–1)	Bird Index	Percent progress at TS	
				NICS(–1)	Bird Index
		10H-O[b]			
$\bar{C}H_2CN$	–19.8	–3.89	28.99	33.3	35.9
$\bar{C}H_2CO_2H$	–14.3	–4.70	32.58	52.1	56.3
$\bar{C}H_2COCH_3$	–13.0	–4.64	32.81	50.7	57.6
$\bar{C}H_2CHO$	–10.4	–4.99	34.04	59.0	64.6
$\bar{C}H_2NO_2$	–1.2	–4.92	33.34	57.3	60.6
$CH_3\bar{C}HNO_2$	–0.9	–4.76	34.04	53.5	64.6
$\bar{C}H_2(CN)_2$	19.8	–5.04	33.89	60.2	63.7
		10H-S[c]			
$\bar{C}H_2CN$	–26.5	–3.71	42.46	25.9	33.9
$\bar{C}H_2CHO$	–17.1	–4.69	48.19	46.0	51.3
$\bar{C}H_2NO_2$	–7.9	–4.92	48.91	50.7	53.5
$\bar{C}H_2NO$	–0.3	–5.43	54.17	61.0	69.5
$\bar{C}H_2CHS$	1.3	–5.55	53.79	63.6	68.3
$\bar{C}H(CN)_2$	13.1	–5.03	51.31	52.9	60.8
$\bar{C}H(NO_2)_2$	24.7	–5.42	53.08	60.8	66.2

[a]AtMP2/6-31+*G***, ref. [26].
[b]**10H-O/10⁻-O**: NICS(–1) –2.47/–6.74, Bird Index 22.68/40.28.
[c]**10H-S/10⁻-S**: NICS(–1) –2.45/–7.33, Bird Index 31.31/64.20.

Additional confirmation of early development of aromaticity as the reaction progresses comes from plots of NICS values and Bird Indices vs. the reaction coordinate for the reactions of **10H-O** with $\bar{C}H_2NO_2$ (Figs. 2 and 3) and of **10H-S** with $\bar{C}H_2NO$ (Figs. 4 and 5). These reactions were chosen because they are nearly thermoneutral (see Table 9) and have fairly symmetrical transition state as indicated by the C···H···B bond lengths [26]. The plots show a steep rise in aromaticity as a function of the reaction coordinate as the transition state is reached and a pronounced leveling off toward the value of the anionic product once the transition state has been traversed. As indicated in Table 9, the % progress in the development of product aromaticity at the transition state of the reaction of **10H-O** with $\bar{C}H_2NO_2$ is 57.3 for NICS(–1) and 60.6 for the Bird Index, while for the reaction of **10H-S** with $\bar{C}H_2NO$ these percentages are 61.0 and 69.5, respectively.

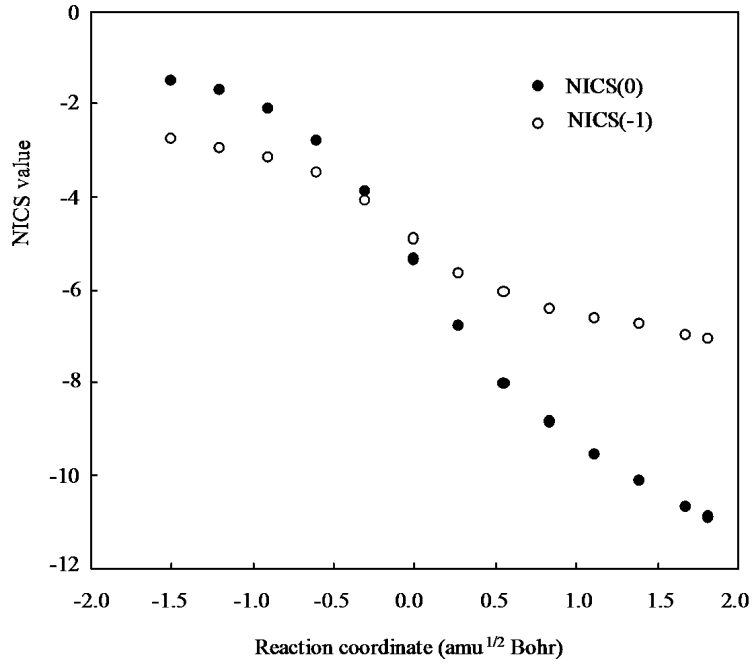

Fig. 2 Plots of NICS(0) and NICS(–1) vs. IRC for the reaction of **10H-O** with $\bar{C}H_2NO_2$.

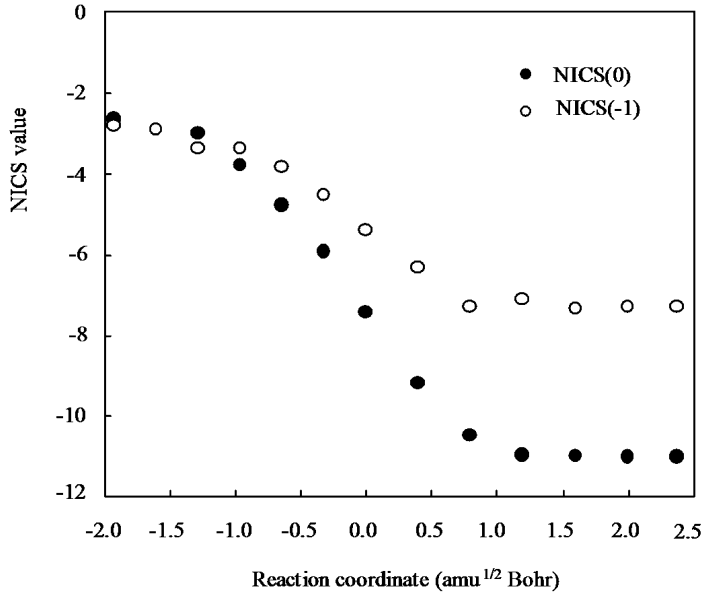

Fig. 3 Plots of NICS(0) and NICS(–1) vs. IRC for the reaction of **10H-S** with $\bar{C}H_2NO$.

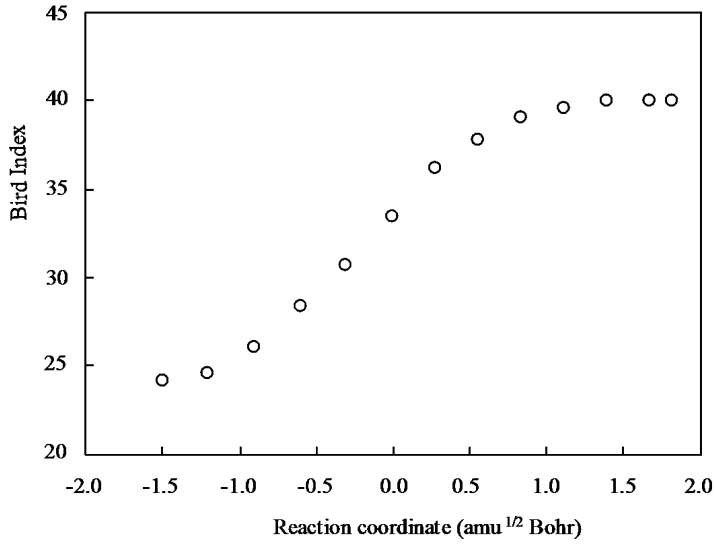

Fig. 4 Plots of the Bird Index vs. IRC for the reaction of **10H-O** with $\bar{C}H_2NO_2$.

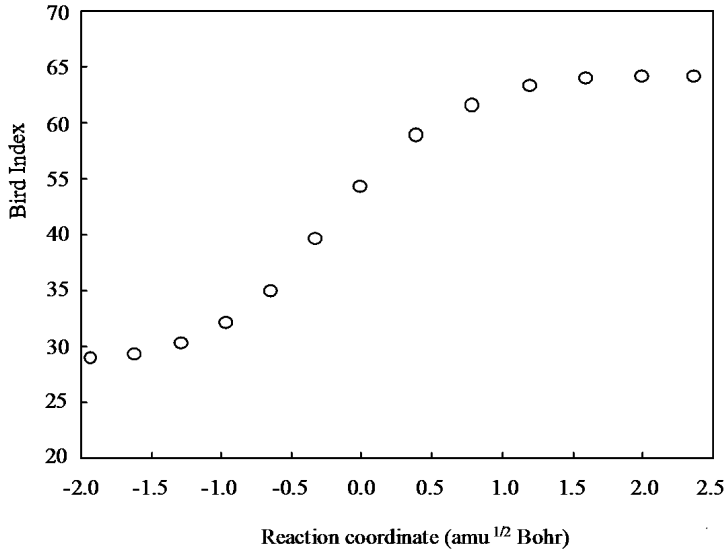

Fig. 5 Plots of the Bird Index vs. IRC for the reaction of **10H-S** with $\bar{C}H_2NO$.

Decoupling of aromaticity development from charge delocalization

In solution-phase reactions such as eq. 1 as well in the gas-phase reactions of eq. 4 charge delocalization always lags behind proton transfer at the transition state. For the solution-phase reactions, this feature not only manifests itself in enhanced intrinsic barriers but also in the Brønsted coefficients. For the gas-phase reactions, this lag can be deduced from calculated NPA charges. An interesting question is whether in systems such as eqs. 8a, 9a, or 10 the early development of aromaticity would induce charge delocalization to follow its pattern rather than the typical pattern of delayed charge delocalization found in non-aromatic systems. NPA charges for some representative systems are shown in Chart 1. They in-

dicate that negative charge is being created at the reaction site of the transition state, which then either disappears ($C_6H_7^+/C_6H_6$ system) or decreases ($C_5H_6/C_5H_5^-$ system) due to delocalization in the product. This implies that the transition state is imbalanced in the same way as in non-aromatic systems, i.e., development of aromaticity and charge delocalization are decoupled.

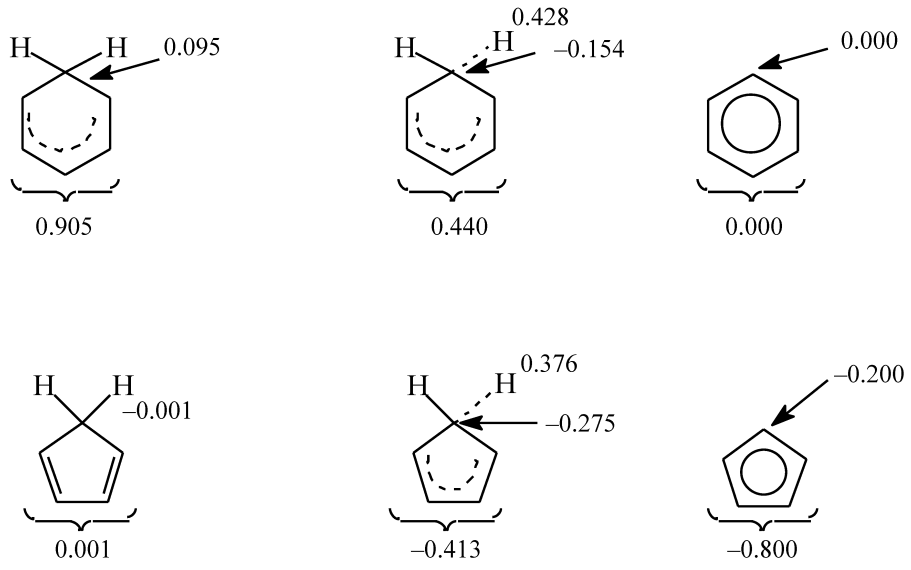

Chart 1

Comparison with aromatic transition states in other reactions

Aromatic transition states are well known, especially in pericyclic reactions such as Diels–Alder and similar processes [28,29]. However, in these reactions aromaticity is a special characteristic of the transition state, whereas reactants and products are not aromatic or much less so. Hence, in these cases it is not a matter of how much of the aromaticity of reactants or products is expressed in the transition state, i.e., the PNS does not apply here. An analogy with steric effects on intrinsic barriers may illustrate the point. In a reaction of the type of eq. 12, steric effect may increase the barrier if the molecules are

$$A+B \rightleftharpoons C+D \tag{12}$$

bulky. However, because there are no steric effects on the reactants or products, the question of how much of reactant/product steric effects is expressed in the transition state does not apply. This contrasts with a reaction of the type of eq. 13 where there is potential steric crowding both at the transition state

$$A+B \rightleftharpoons AB \tag{13}$$

and in the product. Hence, the PNS does apply here; for example, if the steric effect on the transition state is disproportionately strong, the intrinsic barrier will increase.

Aromaticity vs. resonance

Why does aromaticity and resonance affect intrinsic barriers differently? The lowering of the barrier by providing the transition state with excess aromatic stabilization appears to be in keeping with Nature's principle of always choosing the lowest energy path. The fact that the transition states are able to be so highly aromatic suggests that only relatively minor progress in the creation of appropriate orbitals, or

the establishment of their optimal alignment and distances from each other may be required for aromatic stabilization to become effective. There are several precedents that support this notion. For example, the NICS value of Kekulé benzene (r_{cc} fixed at 1.350 and 1.449 Å) is only 0.8 ppm less than the NICS value for benzene itself or, with r_{cc} = 1.33 Å (ethylene-like) and 1.54 (ethane-like), the NICS value is only 2.6 ppm less than that for benzene [25]. Or, the NICS value for **12** (–8.1 ppm) [30] is quite close to that of benzene (–9.7 ppm) [25] even though there is strong bending of the benzene ring. Other relevant observations have been discussed elsewhere [23].

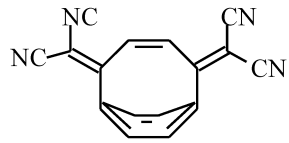

12

In contrast, in reactions that lead to resonance stabilized/delocalized products such as eqs. 1 or 4, the transition state is not able to take advantage of the potentially stabilizing effect of extensive charge delocalization. This is because delocalization can only occur if there is significant C–Y π-bond formation. Hence, the fraction of charge on Y at the transition state depends on the fraction of π-bond formation, which in turn depends on the fraction of charge transferred from the base to the carbon acid. This imposes an insurmountable constraint on the transition state because the charge on Y can never be large since it is a fraction of a fraction.

CONCLUSIONS

- Aromaticity in a product or reactant lowers the intrinsic barrier of proton transfers. This is true for solution-phase as well as gas-phase reactions and contrasts with resonance/charge delocalization which raises the intrinsic barrier.
- Based on the PNS, the lowering of the intrinsic barrier implies that aromaticity runs ahead of proton transfer at the transition state, a conclusion that is confirmed by the calculation of aromaticity indices such as NICS, HOMA, and the Bird Index.
- The high aromaticity of the transition state suggests that only relatively minor progress in the creation or optimal alignment of the relevant orbitals is required for aromatic stabilization to become disproportionately effective. This allows the reaction to lower its barrier. In non-aromatic delocalized systems there is an insurmountable constraint on how much charge delocalization can occur at the transition state, and hence the reaction cannot take advantage of a potentially barrier-lowering effect of advanced delocalization.
- The reasons for the high transition state aromaticity in proton transfers are different from those for the transition state aromaticity in pericyclic reactions. In the former case, it is a matter of what fraction of reactant or product aromaticity is expressed in the transition state and therefore falls under the purview of the PNS. On the other hand, in the latter case one is dealing with a unique property of the transition state that is not related to reactants or products, and hence the PNS does not apply.
- The calculation of NPA group charges indicates that even in aromatic systems charge delocalization lags behind proton transfer in the usual way observed for non-aromatic systems. This means that the development of aromaticity and charge delocalization at the transition state are decoupled.

ACKNOWLEDGMENT

This work has been supported by Grant CHE-0446622 from the National Science Foundation.

REFERENCES

1. R. A. Marcus. *J. Phys. Chem.* **72**, 891 (1968).
2. J. R. Keeffe, A. J. Kresge. In *Investigation of Rates and Mechanisms of Reactions*, C. F. Bernasconi (Ed.), Part 1, p. 747, Wiley-Interscience, New York (1986).
3. (a) C. F. Bernasconi. *Acc. Chem. Res.* **20**, 301 (1987); (b) C. F. Bernasconi. *Acc. Chem. Res.* **25**, 9 (1992); (c) C. F. Bernasconi. *Adv. Phys. Org. Chem.* **27**, 119 (1992).
4. (a) C. F. Bernasconi, W. Sun, L. García-Río, Kin-Yan, K. W. Kittredge. *J. Am. Chem. Soc.* **119**, 5583 (1997); (b) C. F. Bernasconi, M. Ali. *J. Am. Chem. Soc.* **121**, 3039 (1999); (c) C. F. Bernasconi, W. Sun. *J. Am. Chem. Soc.* **124**, 2799 (2002); (d) C. F. Bernasconi, M. Ali, J. G. Gunter. *J. Am. Chem. Soc.* **125**, 151 (2003); (e) C. F. Bernasconi, D. Fairchild, R. L. Montañez, P. Aleshi, H. Zheng, E. Lorance. *J. Org. Chem.* **70**, 7721 (2005); (f) C. F. Bernasconi, M. L. Ragains. *J. Organomet. Chem.* **690**, 5616 (2006).
5. (a) F. Terrier, J. Lelièvre, A.-P. Chatrousse, P. Farrell. *J. Chem. Soc., Perkin Trans. 2* 1479 (1985); (b) F. Terrier, H.-Q. Xie, J. Lelièvre, T. Boubaker, P. G. Farrell. *J. Chem. Soc., Perkin Trans. 2* 1899 (1990); (c) G. Moutiers, B. El Fahid, A.-G. Collet, F. Terrier. *J. Chem. Soc., Perkin Trans. 2* 49 (1996); (d) G. Moutiers, B. El Fahid, R. Goumont, A.-P. Chatrousse, F. Terrier. *J. Org. Chem.* **61**, 1978 (1996).
6. (a) J. B. Nevy, D. C. Hawkinson, G. Blotny, X. Yao, R. M. Pollack. *J. Am. Chem. Soc.* **119**, 12722 (1997); (b) X. Yao, M. Gold, R. M. Pollack. *J. Am. Chem. Soc.* **121**, 6220 (1999).
7. Z. Zhong, T. S. Snowden, M. D. Best, E. V. Anslyn. *J. Am. Chem. Soc.* **126**, 3488 (2004).
8. Nucleophilic addition to alkenes: (a) C. F. Bernasconi. *Tetrahedron* **45**, 4017 (1989); (b) C. F. Bernasconi, R. J. Ketner, M. L. Ragains, X. Chen, Z. Rappoport. *J. Am. Chem. Soc.* **123**, 2155 (2001); (c) C. F. Bernasconi, R. J. Ketner, X. Chen, Z. Rappoport. *ARKIVOC* (xii), 161 (2002).
9. Formation of carbocations: (a) J. P. Richard. *J. Am. Chem. Soc.* **111**, 1455 (1989); (b) J. P. Richard. *J. Org. Chem.* **59**, 25 (1994); (c) J. P. Richard, T. L. Amyes, M. M. Toteva. *Acc. Chem. Res.* **34**, 981 (2001).
10. Reactions of Fischer carbene complexes: (a) C. F. Bernasconi. *Chem. Soc. Rev.* **26**, 299 (1997); (b) C. F. Bernasconi. *Adv. Phys. Org. Chem.* **37**, 13 (2002).
11. Formation of radicals: C. Costentin, J.-M. Saveant. *J. Phys. Chem.* **109**, 4125 (2005).
12. (a) D. A. Jencks, W. P. Jencks. *J. Am. Chem. Soc.* **99**, 7948 (1977); (b) W. P. Jencks. *Chem. Rev.* **85**, 511 (1985).
13. F. G. Bordwell, W. J. Boyle Jr. *J. Am. Chem. Soc.* **94**, 3907 (1972).
14. C. F. Bernasconi, D. Wiersema, M. W. Stronach. *J. Org. Chem.* **58**, 217 (1993).
15. R. P. Bell, S. Grainger. *J. Chem. Soc., Perkin Trans. 2* 1367 (1976).
16. C. F. Bernasconi, P. J. Wenzel. *J. Am. Chem. Soc.* **118**, 11446 (1996).
17. C. F. Bernasconi, D. E. Fairchild. *J. Phys. Org. Chem.* **5**, 409 (1992).
18. C. F. Bernasconi, P. J. Wenzel. *J. Org. Chem.* **66**, 968 (2001).
19. C. F. Bernasconi, K. W. Kittredge. *J. Org. Chem.* **63**, 1944 (1998).
20. C. F. Bernasconi. M. L. Ragains, S. Bhattacharya. *J. Am. Chem. Soc.* **125**, 12328 (2003).
21. C. F. Bernasconi, M. Pérez-Lorénzo. *J. Am. Chem. Soc.* **129**, 2704 (2007).
22. C. F. Bernasconi. H. Zheng. *J. Org. Chem.* **71**, 8203 (2006).
23. C. F. Bernasconi, P. J. Wenzel, M. L. Ragains. *J. Am. Chem. Soc.* **130**, 4934 (2008).
24. T. M. Krygowski, M. Cyranski. *Chem. Rev.* **101**, 1385 (2001).

25. (a) P. v. R. Schleyer, C. Maerker, A. Dransfeld, H. Jiao, W. J. R. van Eikema Hommes. *J. Am. Chem. Soc.* **118**, 6317 (1996); (b) Z. Chen, C. S. Wannese, C. Corminboeuf, R. Puchta, P. v. R. Schleyer. *Chem. Rev.* **105**, 3842 (2005).
26. C. F. Bernasconi, H. Yamataka, N. Yoshimura, M. Sato. *J. Org. Chem.* **74**, 188 (2009).
27. (a) C. W. Bird. *Tetrahedron* **41**, 1409 (1985); (b) C. W. Bird. *Tetrahedron* **42**, 89 (1986); (c) C. W. Bird. *Tetrahedron* **48**, 335 (1992).
28. (a) M. G. Evans. *Trans. Faraday Soc.* **35**, 824 (1939); (b) M. J. S. Dewar. *The Molecular Orbital Theory of Organic Chemistry*, pp. 316–329, McGraw-Hill, New York (1966); (c) H. Zimmerman. *Acc. Chem. Res.* **4**, 272 (1971).
29. R. Herges, H. Jiao, P. v. R. Schleyer. *Angew. Chem., Int. Ed. Engl.* **33**, 1376 (1994).
30. T. Tsuij, M. Okuyama, M. Ohkita, H. Kawai, T. Suzuki. *J. Am. Chem. Soc.* **125**, 951 (2003).